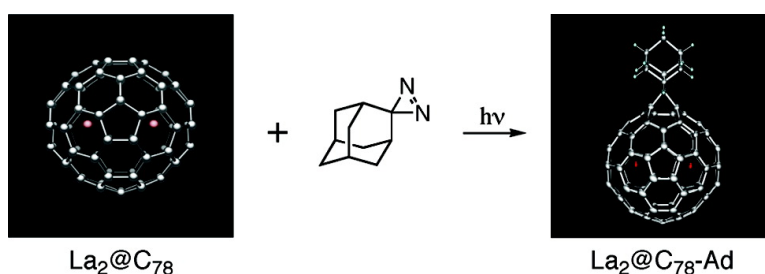Article

Addition of Adamantylidene to La@C: Isolation and Single-Crystal X-ray Structural Determination of the Monoadducts

Baopeng Cao, Hidefumi Nikawa, Tsukasa Nakahodo, Takahiro Tsuchiya, Yutaka Maeda,
Takeshi Akasaka, Hiroshi Sawa, Zdenek Slanina, Naomi Mizorogi, and Shigeru Nagase

$La_2@C_{78}$ $La_2@C_{78}$-Ad

More About This Article

Additional resources and features associated with this article are available within the HTML version:

- Supporting Information
- Links to the 3 articles that cite this article, as of the time of this article download
- Access to high resolution figures
- Links to articles and content related to this article
- Copyright permission to reproduce figures and/or text from this article

View the Full Text HTML

Addition of Adamantylidene to La₂@C₇₈: Isolation and Single-Crystal X-ray Structural Determination of the Monoadducts

Baopeng Cao,[†] Hidefumi Nikawa,[†] Tsukasa Nakahodo,[†] Takahiro Tsuchiya,[†] Yutaka Maeda,[‡,§] Takeshi Akasaka,*,[†] Hiroshi Sawa,[∥] Zdenek Slanina,[†] Naomi Mizorogi,[⊥] and Shigeru Nagase*,[⊥]

Center for Tsukuba Advanced Research Alliance, University of Tsukuba, Tsukuba 305-8577, Japan, Department of Chemistry, Tokyo Gakugei University, Tokyo 184-8501, Japan, PRESTO, Japan Science and Technology Agency, Tokyo 102-0075, Japan, Institute of Materials Structure Science, High-Energy Accelerator Research Organization, Tsukuba 305-0801, Japan, and Department of Theoretical and Computational Molecular Science, Institute for Molecular Science, Okazaki 444-8585, Japan

Received August 28, 2007; E-mail: akasaka@tara.tsukuba.ac.jp; nagase@ims.ac.jp

Abstract: Thermal and photochemical reactions of La₂@C₇₈ with 2-admantane-2,3-[3H]-diazirine are investigated. Four isomers of the monoadduct (La₂@C₇₈Ad) synthesized by the photoreaction are isolated by HPLC and characterized by mass, UV−vis−NIR absorption, cyclic voltammogram and differential pulse voltammogram spectroscopy, proton and ¹³C NMR spectroscopic analysis, single-crystal X-ray diffraction analysis, and theoretical approaches. The addition reactions occur at both the [5,6] and [6,6] positions. X-ray and theoretical studies indicate that one of the monoadduct isomers has an open structure with two La atoms on the C_3 axis of the D_{3h} cage of La₂@C₇₈.

Introduction

It is well-known that incorporation of metallic guest species inside fullerene cages has awarded plentiful, various materials, known as endohedral metallofullerenes, with novel structures and properties that have potential application perspectives associated with the incarcerated metal.[1,2] Endohedral metallofullerenes have therefore attracted much attention in the past decade.[3] Several unstable fullerene cage isomers such as I_h-C₈₀ and C_{2v}-C₈₂ have been stabilized and produced by encaging metal atoms or their clusters.[4−6] Endohedral metallofullerenes make a promise as hosts for radioactive atoms for use in nuclear medicines.[7−8] Because of the inner-molecular electron transfer, the isolated-pentagon-rule violated (IPR-violated) fullerene cages such as C₆₆, C₆₈, and C₇₂ have been synthesized only in the

form of endohedral fullerenes Sc₂@C₆₆,[9] Sc₃N@C₆₈,[10] Sc₂C₂ @C₆₈,[11] La₂@C₇₂,[12] and La@C₇₂−C₆H₃Cl₂.[13] Even for C₇₀ and C₈₄ that have IPR-obeyed cage isomers, metal clusters are encaged in the IPR-violated cage isomers, as found recently for Sc₃N@C₇₀[14] and Tb₃N@C₈₄.[15] Encaging of metal atoms and clusters can modify the reactivity and electrochemical properties of empty fullerenes as well.[1] It has been proved that the reactivity of endohedral metallofullerenes is very different from that of their empty counterparts.[16] Recent studies on endohedral metallofullerenes have focused on their reactivity and functionalization.[17−35] Balch, Dorn, and co-workers have investigated the reaction of 6,7-dimethoxyisochroman-3-one with Sc₃N@C₈₀ and

† University of Tsukuba.
‡ Tokyo Gakugei University.
§ Japan Science and Technology Agency.
∥ High-Energy Accelerator Research Organization.
⊥ Institute for Molecular Science.
(1) Akasaka, T.; Nagase, S., Eds. *Endofullerenes: A New Family of Carbon Clusters*; Kluwer Academic Publishers: Dordrecht, The Netherlands, 2002.
(2) Thilgen, C.; Diederich, F. *Chem. Rev.* **2006**, *106*, 5049.
(3) Dunsch, L.; Yang, S. *Phys. Chem. Chem. Phys.* **2007**, *9*, 3067.
(4) Stevenson, S.; Rice, G.; Glass, T.; Harich, K.; Cromer, F.; Jordan, M. R.; Craft, J.; Hadju, E.; Bible, R.; Olmstead, M. M.; Maitra, K.; Fisher, A. J.; Balch, A. L.; Dorn, H. C. *Nature* **1999**, *401*, 55.
(5) Stevenson, S.; Nagase, S.; Kobayashi, K.; Waelchli, M.; Yamamoto, K.; Funasaka, H.; Kato, M.; Hoshino, T.; Erata, T. *Angew. Chem., Int. Ed. Engl.* **1997**, *36*, 1643.
(6) Akasaka, T. et al. *J. Am. Chem. Soc.* **2000**, *122*, 9316.
(7) Wilson, L. J.; Cagle, D. W.; Thrash, T. P.; Kennel, S. J.; Mirzadeh, S.; Alford, J. M.; Ehrhardt, G. J. *Coord. Chem. Rev.* **1999**, *192*, 199.
(8) Li, Q.; Xiu, Y.; Zhang, X.; Liu, R.; Du, Q.; Shun, X.; Chen, S.; Li, W. *Nucl. Med. Biol.* **2002**, *29*, 707.

(9) Wang, C.; Kai, T.; Tomiyama, T.; Yoshida, T.; Kobayashi, T.; Nishibori, E.; Takata, M.; Sakata, M.; Shinohara, H. *Nature* **2000**, *408*, 426.
(10) Stevenson, S.; Fowler, P. W.; Heine, T.; Duchamp, J.; Rice, G.; Glass, T.; Harich, K.; Hadju, E.; Bible, R.; Dorn, H. C. *Nature* **2000**, *408*, 427.
(11) Shi, Z.; Wu, X.; Wang, C.; Lu, X.; Shinohara, H. *Angew. Chem., Int. Ed.* **2006**, *45*, 2107.
(12) Kato, H.; Taninaka, A.; Sugai, T.; Shinohara, H. *J. Am. Chem. Soc.* **2003**, *125*, 7782.
(13) Wakahara, T.; Nikawa, H.; Kikuchi, T.; Nakahodo, T.; Rahman, G. M. A.; Tsuchiya, T.; Maeda, Y.; Akasaka, T.; Yoza, K.; Horn, E.; Yamamoto, K.; Mizorogi, N.; Slanina, Z.; Nagase, S. *J. Am. Chem. Soc.* **2006**, *128*, 14228.
(14) Yang, S.; Popov, A.; Dunsch, L. *Angew. Chem., Int. Ed. Engl.* **2007**, *46*, 1256.
(15) Beavers, C. M.; Zuo, T.; Duchamp, J. C.; Harich, K.; Dorn, H. C.; Olmstead, M. M.; Balch, A. L. *J. Am. Chem. Soc.* **2006**, *128*, 11352.
(16) Cao, B.; Wakahara, T.; Maeda, Y.; Han, A.; Akasaka, T.; Kato, T.; Kobayashi, K.; Nagase, S. *Chem.−Eur. J.* **2004**, *10*, 705.
(17) Akasaka, T.; Kato, T.; Kobayashi, K.; Nagase, S.; Yamamoto, K.; Funasaka, H.; Takahashi, T. *Nature* **1995**, *374*, 600.
(18) Akasaka, T.; Nagase, S.; Kobayashi, K.; Suzuki, T.; Kato, T.; Yamamoto, K.; Funasaka, H.; Takahashi, T. *J. Chem. Soc., Chem. Commun.* **1995**, 1343.
(19) Akasaka, T.; Kato, T.; Nagase, S.; Kobayashi, K.; Yamamoto, K.; Funasaka, H.; Takahashi, T. *Tetrahedron* **1996**, *52*, 5015.

found that the Diels−Alder addition occurs at a [5,6] ring fusion of C_{80}.[21−22] Echegoyen and co-workers have found that the 1,3-dipolar cycloaddition of azomethine ylide to $M_3N@C_{80}$ (M = Sc, Y) occurs at either [6,6] or [5,6] ring junctions of the C_{80} cage, depending on the M atom.[23−25] For the addition of 1,3-dipolar azomethine ylide to D_{5h}- and I_h-$Sc_3N@C_{80}$, Dorn and co-workers have found that D_{5h}-$Sc_3N@C_{80}$ is more reactive than I_h-$Sc_3N@C_{80}$ and a monoadduct at the [6,6] ring junction is more thermodynamically stable.[26] For the reaction with *N*-triphenylmethyl-5-oxazolidinone via the corresponding azomethine ylide, both the [6,6] and [5,6] pyrrolidine monoadducts of $Sc_3N@C_{80}$ (I_h) have been synthesized and isolated, and it has been found that the kinetically preferred [6,6] adduct is converted into the more thermodynamically stable [5,6] adduct upon refluxing in chlorobenzene.[27] The rearrangement of regioisomers of endohedral metallofullerene derivatives has also been observed by Echegoyen and co-workers.[24] Recent investigations on functionalization of endohedral metallofullerenes have shed light on their applications. Owing to the modified reactivity, some new endohedral metallofullerene derivatives that bear special functional groups have been synthesized and the intriguing properties have been presented. A communication between the dynamic motion of two M atoms within $M_2@C_{80}$ (M = La, Ce) and exohedral groups has been fulfilled by either bis-silylation with 1,1,2,2-tetrakis-(2,4,6-trimethylphenyl)-1,2-disilirane or the [2 + 3] cycloaddition of 1,3-dipolar azomethine ylide.[28,29] Water-soluble functionalized endohedral metallofullerenes, $Gd@C_{60}[C(COOH)_2]$ and $Gd@C_{82}(OH)_x$, have been found to act as effective relaxation MRI (magnetic residence imaging) contrast agents.[30−32] It has been shown that functionalization of an endohedral metallofullerene with diazirine is an efficient way for growth of a single crystal toward a final solution of its structure.[33−34] Missing endohedral metallo-

fullerene $La@C_{74}$ and non-IPR endohedral metallofullerene $La@C_{72}$ exist only in their functionalized forms.[13,35] However, investigations on reactivity and functionalization of endohedral metallofullerenes are mostly focused on the most abundant C_{82}- and C_{80}-cage based species, $M@C_{82}$, $M_2@C_{80}$, and $M_3N@C_{80}$; little attention has been given to those with smaller cages because of their scarcity.[13,30,35] Benefiting from a newly developed method, we have recently isolated a new endohedral metallofullerene, $La_2@C_{78}$, in large quantities.[36] UV−vis-NIR absorption and CV measurement have revealed that the electronic structure of $La_2@C_{78}$ is very different from that of C_{78}. It is also found that $La_2@C_{78}$ differs from $Sc_3N@C_{78}$ in the electronic structure despite the same C_{78}-cage. These drive us to investigate the structure and reactivity of $La_2@C_{78}$. Functionalization of C_{78}-based endohedral metallofullerenes has not been reported yet. Here, we report the thermal and photochemical reactions of $La_2@C_{78}$ and 2-admantane-2,3-[3H]-diazirine (**1**) and the isolation and structure determination of the monoadduct, $La_2@C_{78}Ad$ (Ad = adamantylidene).

Experimental Section

Synthesis and Isolation of $La_2@C_{78}$. $La_2@C_{78}$ was synthesized and isolated as previously reported.[36] Briefly, endohedral La-metallofullerenes were produced by the DC arc discharge method and extracted with 1,2,4-trichlorobezene (TCB) at reflux temperature. The composite graphite rod for burning contains 2% La (Japan Carbon). The arc discharging was performed under 150 Torr of He flow and at 20 V. The arcing current was kept around 35 A. The soot was collected and extracted under Ar atmosphere protection. A controlled-potential bulk reduction of the extract in *o*-DCB solution in the presence of *n*-Bu$_4$-ClO$_4$ (3.0×10^{-2} M) was carried out to selectively reduce the endohedral metallofullerenes into their anions. After removing *o*-DCB, a mixture of acetone/CS$_2$ (4:1 in volume) was added to the system, and the endohedral metallofullerene anions were easily dissolved in the acetone layer because of their good solubility while the abundant empty fullerenes remained in solid form. A moderate oxidant, CHCl$_2$-COOH, was added to the acetone/CS$_2$ extract to oxidize the endohedral metallofullerene anions into neutral species that precipitated from the mixed solvent. The precipitates were then dissolved in toluene for HPLC separation. Both HPLC and mass spectrometric analyses indicate that there is no empty fullerene in the endohedral metallofullerene precipitates. Isolation of $La_2@C_{78}$ was fulfilled by HPLC with a PYE column in a single step (ϕ 20 mm × 250 mm, Nacalai, toluene eluent, 10 mL/min flow rate). The purity of the isolated $La_2@C_{78}$ sample is >99.9%, as confirmed by mass spectroscopic and HPLC analyses.

Reaction of $La_2@C_{78}$ with 1. Diazirine **1** was synthesized and purified as reported in literature.[37] Its purity was estimated to be 99.9% by TLC, ^{1}H and ^{13}C NMR, and mass spectrometry. The thermal reaction of $La_2@C_{78}$ and **1** was carried out in a sealed system under an Ar atmosphere. The bath temperature was kept at 120 ± 2 °C, and the heating time was 30 min. The photochemical reaction was completed in a quartz tube. The radiation wavelength was >300 nm, and the radiation time was 60 s. About 6 mg of the freshly prepared **1** (excess amount, 3.7×10^{-5} mol) was added to 30 mL of 1.1×10^{-4} M $La_2@C_{78}$ (4 mg, 3.2×10^{-6} mol) toluene solution, and the solution was frozen and degassed three times in a liquid-nitrogen-equipped high vacuum line. The $La_2@C_{78}$−admantylidene adducts ($La_2@C_{78}Ad$) were produced, as shown in Scheme 1.

Isolation of $La_2@C_{78}Ad$. Separation and isolation of $La_2@C_{78}Ad$ were carried out by HPLC with a Buckyprep column (ϕ 50 mm × 250

(20) Akasaka, T.; Nagase, S.; Kobayashi, K.; Suzuki, T.; Kato, T.; Kikuchi, K.; Achiba, Y.; Yamamoto, K.; Funasaka, H.; Takahashi, T. *Angew. Chem., Int. Ed. Engl.* **1995**, *34*, 2139.

(21) Lezzi, E. B.; Duchamp, J. C.; Harich, K.; Glass, T. E.; Lee, H. M.; Olmstead, M. M.; Balch, A. L.; Dorn, H. C. *J. Am. Chem. Soc.* **2002**, *124*, 524.

(22) Lee, H. M.; Plmstaed, M. M.; Lezzi, E.; Duchamp, J. C.; Dorn, H. C.; Balch, A. L. *J. Am. Chem. Soc.* **2002**, *124*, 3494.

(23) Cardona, C. M.; Kitaygorodskiy, A.; Echegoyen, L. *J. Am. Chem. Soc.*, **2005**, *127*, 10448.

(24) Cardona, C. M.; Elliott, B.; Echegoyen, L. *J. Am. Chem. Soc.* **2006**, *128*, 6480.

(25) Antonio, R. F.; Campanera, M. J.; Cardona, C. M.; Echegoyen, L.; Polet, J. M. *Angew. Chem., Int. Ed.* **2006**, *45*, 8176.

(26) Cai, T.; Xu, L.; Anderson, M. R.; Ge, Z.; Zuo, T.; Wang, X.; Olmstead, M. M.; Balch, A. L.; Gilbson, H. W.; Dorn, H. C. *J. Am. Chem. Soc.* **2006**, *128*, 8581.

(27) Cai, T.; Slebodnick, C.; Xu, L.; Harich, K.; Glass, T. E.; Chancellor, C.; Fettinger, J. C.; Olmstead, M. M.; Balch, A. L.; Gilbson, H. W.; Dorn, H. C. *J. Am. Chem. Soc.* **2006**, *128*, 6486.

(28) Yamada, M.; Wakahara, Y.; Lian, Y.; Tsuchiya, T.; Waelchli, M.; Mizorogi, N.; Nagase, S.; Kadish, K. M. *J. Am. Chem. Soc.* **2006**, *128*, 1400.

(29) Yamada, M.; Wakahara, Y.; Nakahodo, T.; Tsuchiya, T.; Maeda, Y.; Akasaka, T.; Yoza, T.; Horn, E.; Mizorogi, N.; Nagase, S. *J. Am. Chem. Soc.* **2006**, *128*, 1402.

(30) Bolskar, R. D.; Benedetto, A. F.; Husebo, L. O.; Price, R. E.; Jackson, E. F.; Wallace, S.; Wilson, L. J.; Alford, J. M. *J. Am. Chem. Soc.* **2003**, *125*, 5471.

(31) Mikawa, M.; Kato, H.; Okumura, M.; Narazaki, M.; Kanazawa, Y.; Miwa, N.; Shinohara, H. *Bioconjugate Chem.* **2001**, *12*, 510.

(32) Kato, H.; Kanazawa, Y.; Okumura, M.; Taninaka, A.; Yokokawa, T.; Shinohara, H. *J. Am. Chem. Soc.* **2003**, *125*, 4391.

(33) Iiduka, Y.; Wakahara, T.; Nakahodo, T.; Tsuchiya, T.; Sakuraba, A.; Maeda, Y.; Akasaka, T.; Yoza, K.; Horn, E.; Liu, M. T. H. *J. Am. Chem. Soc.* **2005**, *127*, 12500.

(34) Maeda, Y.; Matsunaga, Y.; Wakahara, T.; Tsuchiya, T.; Ishitsuka, M. O.; Hasegawa, T.; Akasaka, T.; Liu, M. T. H.; Kokura, K.; Horn, E.; Yoza, K.; Kato, T.; Kobayashi, K.; Nagase, S.; Yamamoto, K. *J. Am. Chem. Soc.* **2004**, *126*, 6858.

(35) Nikawa, H.; Kikuchi, T.; Wakahara, T.; Nakahodo, T.; Tsuchiya, T.; Rahman, G. M. A.; Akasaka, T.; Maeda, Y.; Yoza, K.; Horn, E.; Mizorogi, N.; Nagase, S. *J. Am. Chem. Soc.* **2005**, *127*, 9684.

(36) Cao, B.; Wakahara, T.; Tsuchiya, T.; Kondo, M.; Rahman, G. M. A.; Akasaka, T.; Kobayashi, K.; Nagase, S.; Yamamoto, K. *J. Am. Chem. Soc.* **2004**, *126*, 9164.

(37) Liu, M. T. H., Ed. *Chemistry of Diazirines*; CRC Press: Boca Raton, FL, 1987; Vols. 1 and 2.

Scheme 1
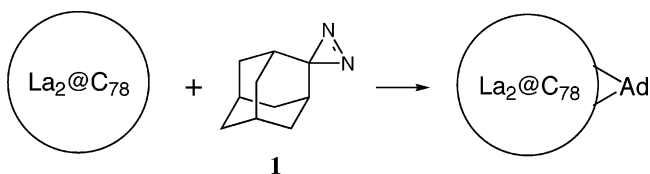
mm, Nacalai, toluene eluent, 10 mL/min flow rate, room temperature). Before injection, the solution was wrapped with aluminum foil for prevention of exposure to the light that could increase the chance of formation of the multiadducts.

Characterization of La₂@C₇₈Ad. The LD-TOF mass spectrum was measured on a BRUKER MALDI BIFLEX III spectrometer (negative mode with 1,1,4,4-tetraphenyl-1,3-butadiene as matrix). UV−vis-NIR absorption spectra were measured on a SHIADZU UV-3150 spectrometer in CS_2 solution at room temperature. ^1H and ^{13}C NMR spectra were obtained at 125 MHz on a BRUKER AVANCE 500 spectrometer equipped with CryoProbe system in CS_2 solution with a capillary of acetone-d_6 as external lock. Details of ^1H and ^{13}C NMR chemical shifts are as follows. M_1: ^{13}C NMR, 146.64 (1C), 146.12 (1C), 146.07(2C), 145.89 (1C), 145.87 (1C) 145.56 (1C), 145.19(2C), 143.49(2C), 142.96 (1C), 142.69(2C), 142.09(2C), 141.52(2C), 141.48(2C), 141.41(6C), 141.40(2C), 141.24(4C), 139.87(2C), 139.79(2C), 138.90(2C), 138.84-(2C), 138.79(2C), 138.57(2C), 137.28(2C), 135.95(2C), 135.90(2C), 135.01(2C), 135.01(2C), 132.99(2C), 132.36(2C), 131.61(2C), 131.61-(2C), 131.46(2C), 130.60(2C), 130.05(2C), 129.01(2C), 127.76(2C), 114.25(2C), 113.81(2C), 71.73(2C). M_3: ^{13}C NMR, 149.87(2C), 149.05(2C), 148.57(1C), 146.32(2C), 146.25(2C), 145.57(2C), 144.83-(2C), 144.79(2C), 144.26(2C), 143.85(2C), 143.68(2C), 143.35(2C), 142.59(2C), 141.88(2C), 141.37(2C), 140.60(1C), 140.05(2C), 139.04-(2C), 138.26(2C), 137.76(2C), 137.69(2C), 137.49(2C), 137.29(2C), 136.28(2C), 136.20(2C), 136.14(2C), 135.86(2C), 135.81(2C), 135.69-(2C), 135.44(2C), 134.80(2C), 134.71(2C), 134.23(2C), 132.48(2C), 130.56(2C), 129.03(2C), 127.02(2C), 125.77(1C), 125.56(1C), 124.97-(2C), 100.49(2C), 61.96(1C), (1C), 35.51(2C), 35.09(2C), 32.74(2C), 32.65(1C), 32.47(1C); ^1H NMR, 3.48 (brd, 2H), 3.39 (brd, 2H), 3.27 (brd, 2H), 2.64 (brd, 1H), 2.62(brd, 1H), 2.02 (brd, 2H), 1.94 (brd, 2H), 1.84 (brd, 2H). M_4: ^{13}C NMR, 166.15(2C), 149.62(2C), 148.75-(1C), 148.32(2C), 146.06(1C), 145.96(2C), 145.48(2C), 144.64(2C), 144.58(2C), 143.07(2C), 141.83(2C), 140.04(2C), 138.02(2C), 137.37-(2C), 136.06(2C), 135.89(2C), 135.54(2C), 134.88(1C), 134.63(2C), 134.52(2C), 134.33(2C), 134.07(2C), 132.95(2C), 132.76(2C), 131.03-(2C), 130.92(2C), 130.84(2C), 130.80(2C), 130.70(2C), 130.59(6C), 129.56(2C), 129.45(2C), 129.21(2C), 128.60(2C), 127.46(1C), 125.71-(2C), 125.09(2C), 114.19(2C), 108.48(2C). 61.94(1C), 39.37(1C), 38.57(2C), 35.07(1C), 34.30(2C), 32.74(2C), 31.08(1C); ^1H NMR, 3.50 (brd, 2H), 3.43 (brd, 2H), 3.34 (brd, 2H), 2.80 (brd, 1H), 2.75 (brd, 1H), 2.62 (brd, 2H), 2.53 (brd, 2H), 1.79 (brd, 2H).

The electrochemical properties (cyclic voltammogram (CV) and differential pulse voltammogram (DPV)) were measured with the Potentiostat/Galvanostat system (BAS CW-50, 0.1 M (n-Bu)₄NPF₆/o-DCB solution, working electrode Pt wire, potentials vs ferrocene/ferrocenium couple). All measurements were performed at a beamline of BL-1A of the Photon Factory, KEK, Japan. X-ray crystallographic analysis was carried out on a BRUKER AXS AMART APEX at 100 K.

Calculations. Geometries of La₂@C₇₈Ad isomers were optimized using the Gaussian 03 program[38] at the B3LYP level[39−41] (ECP[42] and (5s5p3d)/[4s4p3d] for La, and 3-21G for C and H[43] - B3LYP/3-21G∼dz for short). The separation energies and ^{13}C NMR chemical shifts were

(38) Frisch, M. J. et al. *Gaussian 03*, revision C.01; Gaussian Inc.: Wallingford, CT, 2004.
(39) Becke, A. D. *Phys. Rev. A* **1988**, *38*, 3098.
(40) Becke, A. D. *J. Chem. Phys.* **1993**, *98*, 5648.
(41) Lee, C.; Yang, W.; Parr, R. G. *Phys. Rev. B* **1988**, *37*, 785.
(42) Hay, P. J.; Wadt, W. R. *J. Chem. Phys.* **1985**, *82*, 299.

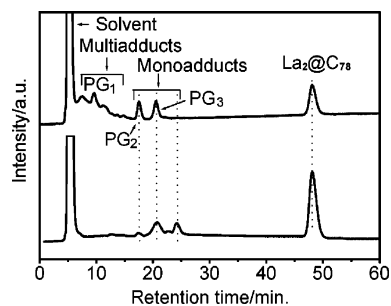**Figure 1.** HPLC analysis on the products of thermal and photochemical reactions of La₂@C₇₈ with **1**. Upper panel: photochemical reaction. Lower panel: thermal reaction.

calculated at the B3LYP/6-31G*∼dz//B3LYP/3-21G∼dz and B3LYP/6-311G*∼dz//B3LYP/3-21G∼dz levels, respectively.

Results and Discussion

Thermal and Photochemical Reactivity of La₂@C₇₈ toward 1. Figure 1 shows the HPLC (Buckyprep column) profiles on the products of thermal and photochemical reactions of La₂@C₇₈ with **1**. As Figure 1 shows, the products of the photochemical reaction are different from those of the thermal reaction. Basically, the photochemical reaction generates three groups of adducts, PG₁, PG₂, and PG₃. Mass spectrometric analyses indicate that PG₁ is ascribed to bis- and even tris-adducts and both PG₂ and PG₃ are monoadducts. Further multistage HPLC analyses with PYE, Buckyclutcher, Buckyprep M, 5PBB, C-18, and Buckyprep columns reveal that PG₂ is a single isomer and PG₃ is composed of three isomers, suggesting that there are four photoactive addition sites for La₂@C₇₈. The photochemical reaction proceeds very fast and is completed in a minute. In the photochemical reaction, multiadducts are easily produced, which contain at least eight bis-adduct isomers, as separated by multistage HPLC with the Buckyprep M column. In contrast, the thermal reaction of La₂@C₇₈ with **1** proceeds slowly to yield basically more than seven monoadduct isomers, in which four isomers are the same as those produced by the photochemical reaction (PG₂ and PG₃), as confirmed by HPLC and UV−vis-NIR spectroscopic analyses. Since the photochemical reaction is somewhat more regioselective than the thermal reaction, we have chosen the photochemical reaction to synthesize the monoadducts, La₂@C₇₈Ad.

Compared with La@C₈₂, La₂@C₈₀, and Sc₃C₂@C₈₀,[33,34] La₂@C₇₈ presents various reactivity toward **1**. La₂@C₈₀ and Sc₃C₂@C₈₀ yield two monoadduct isomers in a ratio of 5:1, showing a high regioselectivity. However, the regioselectivity of La₂@C₇₈ toward **1** is lower.

Mass Spectrometric Identification. Figure 2 shows the LD-TOF mass spectra of La₂@C₇₈Ad measured with 1,1,4,4-tetraphenyl-1,3-butadiene as matrix. In the mass spectrum, only one molecular peak ascribable to La₂@C₇₈Ad is detected, and no fragment from adducts or La₂@C₇₈ is observed, unlike the cases of other endohedral metallofullerene and empty fullerene adducts. It is general that laser-induced cleavage takes place between pristine endohedral metallofullerene and organic addends during the measurement of mass spectra. In some cases, daughter peaks become even more intense than their parents

(43) Binkley, J. S.; Pople, J. A.; Hehre, W. J. *J. Am. Chem. Soc.* **1980**, *102*, 939.
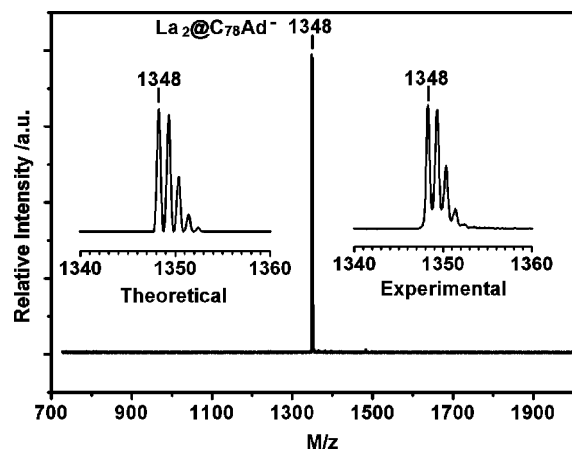(44) Haddon, R. C. *Science* **1993**, *261*, 1545.

Figure 2. LD TOF mass spectrum of $La_2@C_{78}Ad$ (negative mode, 1,1,4,4-tetraphenyl-1,3-butadiene as matrix). Insets: left side − theoretical isotopic distribution, right side − experimental isotopic distribution).
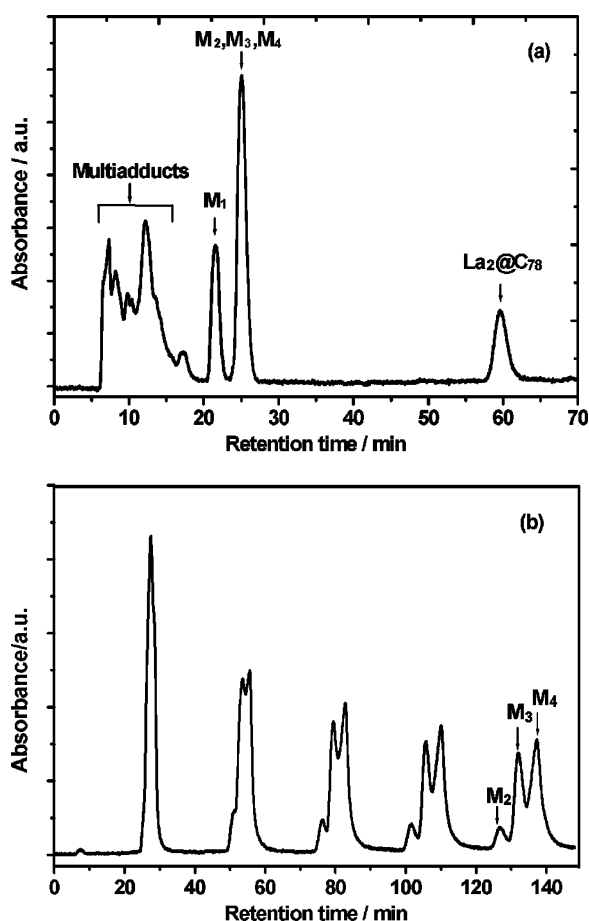

Figure 3. HPLC isolation of $La_2@C_{78}Ad$. (a) Reaction mixture, Buckyprep column. (b) Isolation of M_2, M_3, and M_4 on Buckyprep M column.

because of the bond cleavage between the cage and addend. The fact that no laser-induced fragmentation is found indicates that the binding energy between $La_2@C_{78}$ and Ad is considerably large.

HPLC Isolation and Analyses. The HPLC isolation processes are illustrated in Figure 3. Using the Buckyprep column, isomer M_1 is readily isolated from the other products and starting materials in a single step (cf. Figure 3 panels (a) and support Figure 1) while the other three isomers M_2, M_3, and M_4 overlap with each other with respect to the Buckyprep column, indicating

Table 1. HPLC Retention Times (min) of Four Isomers of $La_2@C_{78}Ad^a$

isomers	Buckyclutcher	Buckyprep	Buckyprep M	5 PYE
M_1	4.35	11.80	12.98	7.98
M_2	4.55	12.25	12.8	8.23
M_3	5.30	12.50	13.4	8.48
M_4	5.23	12.53	13.5	8.45

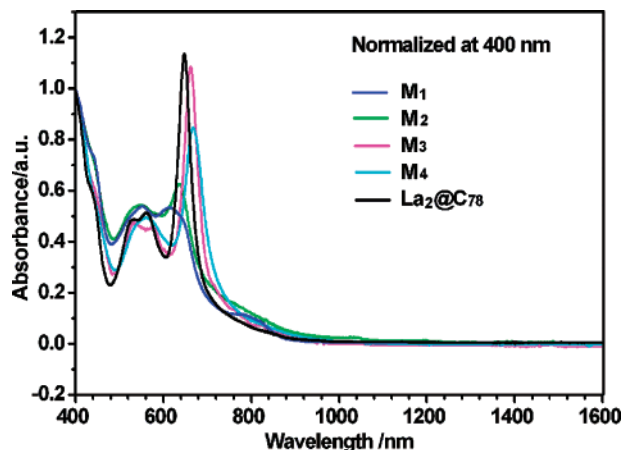^{a} Columns: Nacalai, ϕ 5 mm × 250 mm, toluene eluent, 1.0 mL/min flow rate, 40 °C.

Figure 4. UV−vis−NIR absorption spectra of four isomers of $La_2@C_{78}$-Ad.

Table 2. Absorption Centers of Four Isomers of $La_2@C_{78}Ad$

band	$La_2@C_{78}$	M_1	M_2	M_3	M_4
B_1	533.0	∼520	∼522	531.5	∼535
B_2	562.0	551.5	548.5	577.5	561.5
B_3	648.0	614.0	636.5	662.5	668
B_4		∼790			

the addition position of M_1 is very different from those of M_2, M_3, and M_4. Isolation of the three isomers (a mixture of M_2, M_3, and M_4 in the first stage) was performed in the second stage by recycling HPLC with a Buckyprep M column (Figure 3 panel (b)). HPLC retention times of the four isolated isomers are listed in Table 1. It has been known that the HPLC retention times of isomers of endohedral metallofullerene adducts depend strongly on the cycloaddition positions.[23−25] Isomers M_3 and M_4 show very similar HPLC retention times regardless of columns employed, and their abundances are almost equal, suggesting that they have similar addition positions, as will be below verified by ^{13}C NMR structural analyses.

UV−vis−NIR Absorption. Figure 4 shows the UV−vis−NIR absorption spectra of $La_2@C_{78}Ad$ isomers and $La_2@C_{78}$ in CS_2 solution. For comparison purposes, the absorbances at 400 nm are normalized to unity. Details of absorption centers are listed in Table 2. Addition of adamantylidene to $La_2@C_{78}$ does not modify the absorption onset of $La_2@C_{78}$ but changes the main absorption positions and relative absorbance, though the absorption patterns are basically kept. For absorption spectra, M_3 and M_4 are closer to $La_2@C_{78}$ than M_1 and M_2. As compared with the absorptions of $La_2@C_{78}$, the absorptions of M_3 and M_4 are red-shifted while those of M_1 and M_2 are blue-shifted. These suggest that the addition positions of M_1 and M_3 are similar to those of M_2 and M_4, respectively. M_1 shows an additional distinct absorption around 800 nm, indicating that M_1 differs considerably from $La_2@C_{78}$ in the electronic structure.
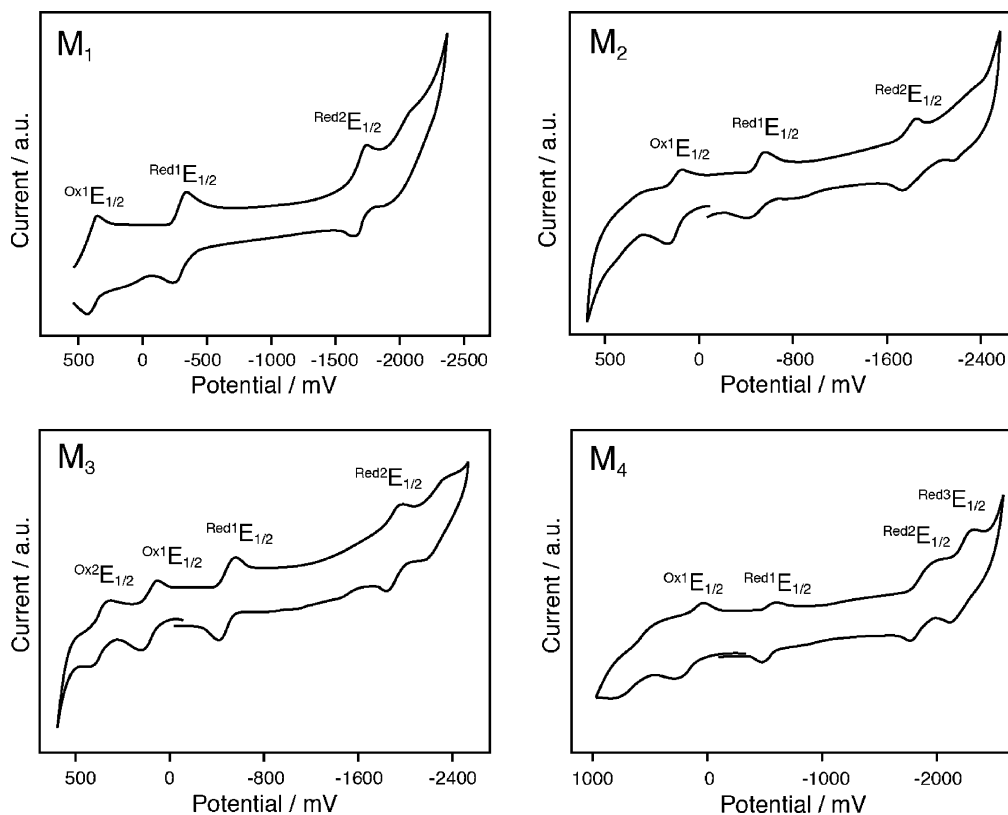
Figure 5. CV of La$_2$@C$_{78}$Ad isomers.

Table 3. Reduction and Oxidation Potentials of La$_2$@C$_{78}$Ad Isomers Based on DPV Measurements

	M$_1$	M$_2$	M$_3$	M$_4$	La$_2$@C$_{78}$
$^{Ox2}E_{1/2}$	0.63	0.69	0.61	0.63	0.62
$^{Ox1}E_{1/2}$	0.23	0.16	0.21	0.13	0.26
$^{Red1}E_{1/2}$	−0.43	−0.46	−0.48	−0.44	−0.40
$^{Red2}E_{1/2}$	−1.82	−1.83	−1.83	−1.78	−1.84

Electrochemical Properties. Figure 5 shows the CV profiles measured from 900 to 2400 mV for M$_1$, M$_2$, M$_3$, and M$_4$ in *o*-dichlorobenzene solution. All the monoadducts present clear reversible CV peaks, indicating that the reduction and oxidation are reversible. The third reduction peak is not as clear as the others because of the strong background response. As is apparent from the reduction and oxidation DPV potentials listed in Table 3, the first reduction and oxidation potentials of La$_2$@C$_{78}$Ad isomers are slightly negatively shifted, with respect to La$_2$@C$_{78}$, indicating that the adducts are somewhat more readily oxidized than La$_2$@C$_{78}$.

^{1}H and ^{13}C NMR Structural Analyses. The ^{13}C NMR spectrum of M$_1$ presents a total of 42 lines (36 (full intensity) + 6 (half intensity)) in the region of 170−80 ppm. In addition, 7 lines (3 (full intensity) + 4 (half intensity)) were observed for the adamantane group. The ^{13}C NMR spectra of M$_1$ disclose that M$_1$ has C_s symmetry. The ^{13}C NMR spectra of M$_3$ and M$_4$ show 41 lines (37 (full intensity) + 4 (half intensity)) in the field of 170−100 ppm and similar patterns observed for M$_1$ in the adamantane region, indicating that M$_3$ and M$_4$ have C_s symmetry, as also confirmed by their ^{1}H NMR spectroscopic analyses. The details of ^{13}C and ^{1}H NMR chemical shifts are listed in the Experimental Section.

Single-Crystal X-ray Structural Analysis. It has been found from single-crystal X-ray structural analysis that the Sc$_3$N cluster in Sc$_3$N@C$_{78}$ cocrystallized with porphyrin is located on the central σ_h mirror plane of the D_{3h}-C$_{78}$.[45,46] However, it was found to be of critical difficulty to obtain a single crystal of La$_2$@C$_{78}$ without coordination or derivatization because of its sphere shape. Here, we have succeeded in preparing a good single crystal of La$_2$@C$_{78}$Ad suitable for single-crystal X-ray structural analysis.

Black, needle-like single crystals of La$_2$@C$_{78}$Ad were obtained by slow volatilization of solvent from a solution of La$_2$@C$_{78}$Ad in CS$_2$ using an upper layer of hexane to prevent fast evaporation. Isomer M$_1$ was employed for crystallization since it can be readily isolated in a large amount in a single step. The size of the single crystal utilized for X-ray diffraction is around $0.2 \times 0.1 \times 0.1$ mm^3. Figure 6 shows the structure of M$_1$ with 80% occupancy determined by single-crystal X-ray diffraction analysis at 100 K (crystal system: hexagonal, space group: $P_{63/m}$, lattice parameters: $a = 26.564$ (2) Å, $b = 26.564$ (2) Å, $c = 10.8869$ (9) Å, $\alpha = 90°$, $\beta = 90°$, $\gamma = 120°$). As is obvious from Figure 6, the addition of adamantylidene to La$_2$@C$_{78}$ takes place at the [5,6] junction that is perpendicular to the central σ_h mirror plane and parallel to the C_3 axis of the D_{3h}-C$_{78}$ cage. La$_2$@C$_{78}$Ad (M$_1$) has C_s symmetry, as indicated by ^{13}C and ^{1}H NMR analyses. The C−C bond attached by Ad is elongated to 1.886 Å. This distance is much longer than the typical C−C single bond distances, indicating that La$_2$@C$_{78}$-Ad (M$_1$) has an opened structure. Similar opened structures have been also observed for La@C$_{82}$Ad and C$_{60}$CF$_2$.[34,47]

(45) Olmstead, M. M.; des Bettencourt-Dias, A.; Duchamp, J. C.; Stevenson, S.; Marcui, D.; Dorn, H. C.; Balch, A. L. *Angew. Chem., Int. Ed.* **2001**, *40*, 1223.
(46) Campanera, J. M.; Bo, C.; Olmstead, M. M.; Balch, A. L.; Poblet, J. M. *J. Phys. Chem. A* **2002**, *106*, 12356.
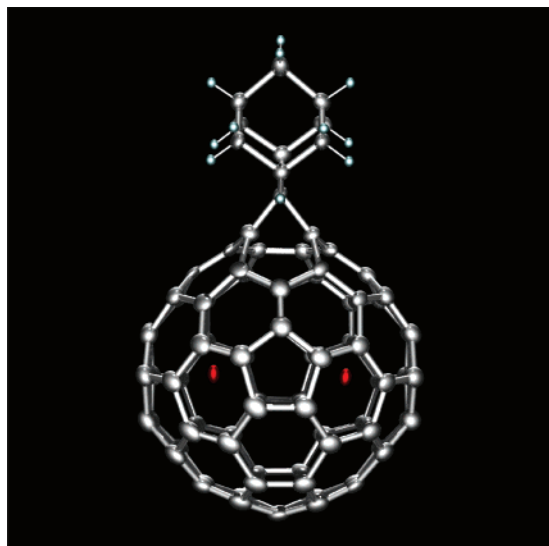
Figure 6. ORTEP drawing of the structure of $La_2@C_{78}Ad$ (M_1) determined by single-crystal X-ray diffraction structural analysis. Only the major La−La orientation with 80% occupancy is displayed.
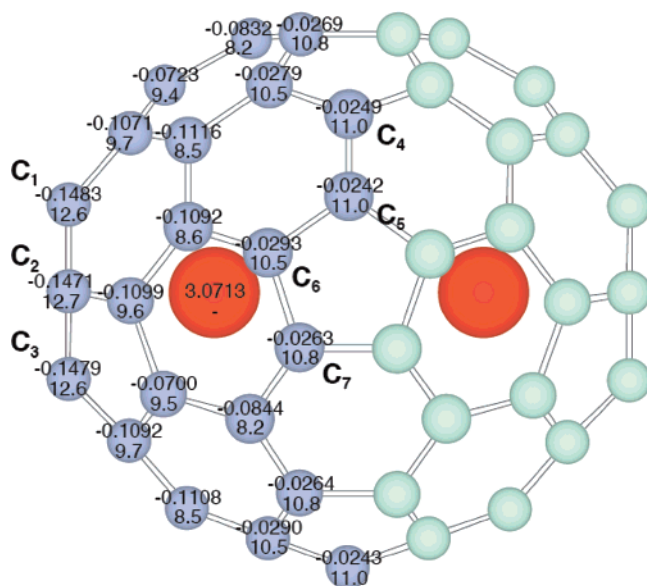

Figure 8. Structures of $La_2@C_{78}Ad$ (M_1): (a) X-ray crystal structure of the most occupied orientation; (b) corresponding DFT optimized structure; (c and d) DFT optimized disordered structures.

Figure 7. Charge densities (upper values) and POAV (lower values) of $La_2@C_{78}$.

In the single-crystal X-ray structural analyses, three La_2 pairs were observed to be disordered with occupation percentages 80%, 10%, and 10%, respectively. As shown in Figure 6, two La atoms are located on the C_3 axis of the D_{3h}-C_{78} cage with a La−La distance of 4.081 Å for the highest occupation percentage. This agrees with the positions of two La atoms determined previously for the pristine $La_2@C_{78}$ on the ^{13}C NMR time scale.[36]

Theoretical Analysis. The calculated charge densities and p-orbital axial vector (POAV) values[44] of $La_2@C_{78}$ are shown in Figure 7. Three carbons with the largest density and POAV terms (C_1, C_2, and C_3) are located around the C_3 symmetry axis (polar region). Addition in this region would result in the [5,6]
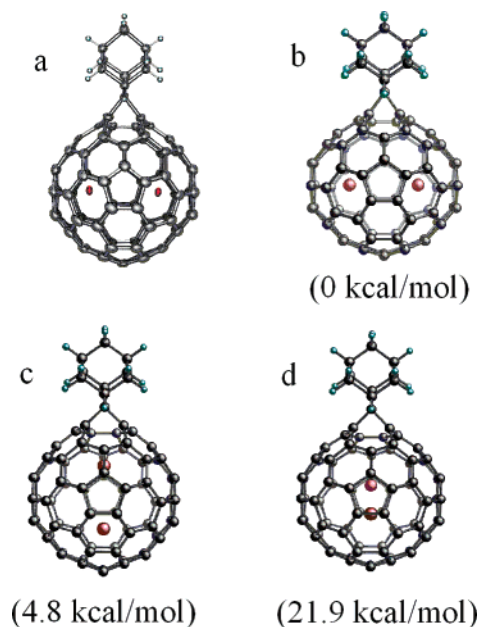
(47) Pimenova, A. S.; Kozlov, A. A.; Goryunkov, A. A.; Markov, V. Y.; Khavrel, P. A.; Avdoshenko, S. M.; Ioffe, I. N.; Sakharov, S. G.; Troyanov, S. I. Sidorov, L. N. *Chem. Commun.* **2007**, 374.

or [6,6] adduct with C_s symmetry, exhibiting 41 ^{13}C NMR lines from the cage carbons (37(full intensity) + 4(half intensity)). Another region with high POAV values is formed by C_4, C_5, C_6, and C_7 (equator belt), suggesting three [5,6] and one [6,6] adducts - two C_1, one C_s, and one with C_{2v} symmetry, possessing 78 lines, 42 lines (36(full intensity) + 6(half intensity)), and 22 lines (17(full intensity) + 5(half intensity)), respectively, in the fullerene region ^{13}C NMR spectra. The theoretical results are in line with the ^{13}C and ^1H NMR spectra and X-ray single-crystal diffraction. We have isolated four monoadduct isomers, three of which (major isomers) have been determined on the basis of ^{13}C NMR analysis to have C_s symmetry while the last one still remains unclear because of its low production yield. One of the C_s symmetric adducts (M_1) has been clearly proven by X-ray diffraction to be the [5,6] addition product in the equator region.

Since three orientations of the two encased La atoms are observed for M_1 in X-ray single-crystal diffraction, we optimized the three structures (Figure 8). It is found that the most stable optimized structure (b) has the two La atoms located on the C_3 axis of the D_{3h}-C_{78} and is open, i.e., the same pattern as that in the X-ray structure (a). This structure (b) is more stable by 4.8 and 21.9 kcal/mol, respectively, than the orientations from the disordered structures (c) and (d). The occupancies of these disordered structures are too low to be detected by ^{13}C NMR. In the optimized structure (b), the length of the [5,6] addition junction is 1.745 Å, which is in agreement with the X-ray value of 1.806 Å. The two La atoms are separated by 3.954 Å, which is also consistent with the X-ray length of 4.081 Å obtained in X-ray analysis as well.

We also performed computation on the theoretical ^{13}C NMR for M_1 on the basis of its X-ray structure. The computed NMR data are in agreement with our measured spectra in terms of chemical shifts and relative intensity pattern. (See Figure S2 in the Supporting Information.)

Conclusions

La$_2$@C$_{78}$ has the larger number of reactive sites than La@C$_{82}$ and La$_2$@C$_{80}$ toward diazirine **1** and yields the larger number of monoadduct isomers. This trend is more enhanced for the thermal reaction than for the photoreaction. Three isomers isolated for La$_2$@C$_{78}$Ad have C_s symmetry. The addition occurs at both [5,6] and [6,6] junctions around the pole and equator of La$_2$@C$_{78}$. The electronic structure and properties of La$_2$@C$_{78}$ are significantly modified by the addition of Ad. X-ray single-crystal diffraction reveals that one of the isomers has an open structure with two La atoms on the C_3 axis of La$_2$@C$_{78}$ (D_{3h}).

Supporting Information Available: HPLC isolation of M1, complete refs 6 and 38, and experimental and calculated ^{13}C NMR of the monoadducts. This material is available free of charge via the Internet at http://pubs.acs.org.

JA076462V